polymers

MDPI

Article

Poly(3,3-dibenzyl-3,4-dihydro-2*H*-thieno[3,4-*b*][1,4] dioxepine)/Platinum Composite Films as Potential Counter Electrodes for Dye-Sensitized Solar Cells

Jung-Chuan Chou [1,2], Yu-Chi Huang [3], Tzi-Yi Wu [3,*], Yi-Hung Liao [4], Chih-Hsien Lai [1,2], Chia-Ming Chu [2] and Yu-Jen Lin [1]

1 Graduate School of Electronic Engineering, National Yunlin University of Science and Technology, Yunlin 64002, Taiwan; choujc@yuntech.edu.tw (J.-C.C.); chlai@yuntech.edu.tw (C.-H.L.); m10313328@gmail.com (Y.-J.L.)
2 Department of Electronic Engineering, National Yunlin University of Science and Technology, Yunlin 64002, Taiwan; B10113114@yuntech.edu.tw
3 Graduate School of Chemical and Materials Engineering, National Yunlin University of Science and Technology, Yunlin 64002, Taiwan; M10415019@yuntech.org.tw
4 Department of Information and Electronic Commerce Management, TransWorld University, Yunlin 64063, Taiwan; liaoih@twu.edu.tw
* Correspondence: wuty@yuntech.edu.tw; Tel.: +886-5-534-2601 (ext. 4626)

Academic Editor: Chih-Feng Huang
Received: 28 April 2017; Accepted: 3 July 2017; Published: 7 July 2017

Abstract: In this study, poly(3,3-dibenzyl-3,4-dihydro-2*H*-thieno[3,4-*b*][1,4]dioxepine)/platinum composite films (PProDOT-Bz_2/Pt) were used as counter electrodes (CEs) in dye-sensitized solar cells (DSSCs). The composite films were prepared on fluorine-doped tin oxide (FTO) glass by radio frequency (RF) sputtering to deposit platinum (Pt) for 30 s. Afterwards, PProDOT-Bz_2 was deposited on the Pt–FTO glass via electrochemical polymerization. The electron transfer process of DSSCs was investigated using electrochemical impedance spectroscopy (EIS) and cyclic voltammetry (CV). The DSSCs with 0.05 C/cm^2 PProDOT-Bz_2-Pt composite films showed an open circuit voltage (V_{oc}) of 0.70 V, a short-circuit current density (J_{sc}) of 7.27 mA/cm^2, and a fill factor (F.F.) of 68.74%. This corresponded to a photovoltaic conversion efficiency (η) of 3.50% under a light intensity of 100 mW/cm^2.

Keywords: dye-sensitized solar cells; electrochemical impedance spectroscopy; conducting polymer; photovoltaic conversion efficiency

1. Introduction

Dye-sensitized solar cells (DSSCs) are typical photoelectrochemical cells; their efficiencies are comparable to those of traditional p-n junction solar cells. DSSCs have attracted considerable interest due to their low cost of production, environmental friendliness, and low energy consumption [1–8]. The CE is an essential component of DSSCs; it injects electrons into the electrolyte to catalyze the reduction reaction from triiodide ion to iodide ion after a charge injection from the dye [9]. In this regard, Pt has excellent electrical conductivity and high catalytic activity, making it suitable for use as a CE. However, the platinum electrode suffers several challenges: (i) Platinum is expensive and the quantity of platinum worldwide is too small to supply the increasing demands for several fields involving catalysis; (ii) platinum electrodes are easily eroded by iodine-based electrolytes, which will create by-products like PtI_4 and H_2PtI_6 in liquid-state DSSCs; (iii) Pt as a CE in DSSCs is not effective for the I-free redox couple (such as Co^{3+}/Co^{2+} and T_2/T^-) electrolyte; (iv) Pt electrode can be poisoned by sulfur or phosphate species; (v) the platinum electrode cannot match the novel materials of working electrodes, novel

dyes, and novel electrolytes in emerging solar cells. These shortcomings of Pt influence CE stability significantly and give rise to degenerated solar cell performance [10,11]. Conducting polymers (CPs) are promising CEs due to their ease of processing from a solution, CPs have excellent catalytic activity in the metallic state and show great potential to produce large-area and low-cost CEs. In recent years, polyaniline (PANI) [12,13], polypyrrole (PPy) [14], poly(3,4-ethylenedioxythiophene) (PEDOT) [15–18], poly(3,4-ethylenedioxythiophene):poly(4-styrenesulfonate) (PEDOT:PSS) [19–21], polythiophene (PTh) [10], and poly(3,3-diethyl-3,4-dihydro-2*H*-thieno-[3,4-*b*][1,4]-dioxepine) (PProDOT-Et_2) [21,22] have been reported as potential CEs of DSSCs. Moreover, DSSCs using CP-based electrolytes have many benefits associated with solvent-free devices such as improved long-term stability, high thermal stability, low liquid leakage, and so forth [23–30]. However, the applications of poly(3,3-dibenzyl-3,4-dihydro-2*H*-thieno[3,4-*b*][1,4]dioxepine) (PProDOT-Bz_2) in CE of DSSCs are not reported so far. In the present work, cell performances of the DSSCs assembled based on the prepared PProDOT-Bz_2/Pt composite films as CEs were characterized. The authors anticipate that this work will stimulate further scientific research and finally be beneficial in selecting suitable CEs to improve the performance of DSSCs in the future.

2. Materials and Methods

2.1. Materials

Titanium dioxide (TiO_2) powder (P25) was purchased from Degussa, Essen, Germany. The P25 was 80% anatase and 20% rutile. The graphene oxide (GO) was purchased from Tokyo Chemical Industry Co., Ltd., Tokyo, Japan. Ruthenium-535 (N3) was purchased from Solaronix, Aubonne, Switzerland. Absolute ethanol was purchased from Katayama Chemical, Osaka, Japan. Acetylacetone (AcAc) was purchased from Acros Organics, Geel, Belgium. Lithium iodide (LiI) and 4-*tert*-butylpyridine (TBP) were purchased from Sigma-Aldrich, St. Louis, MO, USA. Iodine (I_2) was purchased from Riedel-deHaen, Seelze, Germany. 1-propyl-2,3-dimethylimidazolium iodide (DMPII) was purchased from Tokyo Chemical Industry Co., Ltd., Tokyo, Japan. Fluorine-doped tin oxide (FTO) glass substrate was purchased from C.P. Solar, Co., Ltd., Kaohsiung, Taiwan. 3,3-dibenzyl-3,4-dihydro-2*H*-thieno[3,4-*b*][1,4]dioxepine (ProDOT-Bz_2) was synthesized using our previous procedures [31–33].

2.2. Fabrication of PProDOT-Bz_2 Counter Electrodes

The various Pt–FTO glass substrates were prepared by using radio frequency (RF) sputtering system and sputtering Pt for 30 and 360 s onto FTO glass, respectively. The thickness of Pt layer sputtering for 360 s is 90 nm. The sputtering parameters of Ar flow rate, working pressure, and radio frequency sputtering power were kept at 10 sccm, 30 mTorr, and 60 W, respectively. PProDOT-Bz_2/Pt films were prepared by electrochemical polymerization. The electrochemical system comprised 30 s Pt–FTO glass as a working electrode, Pt wire as a counter electrode, and Ag/AgCl as a reference electrode. PProDOT-Bz_2 was synthesized on 30 s Pt–FTO glass using 0.1 M $LiClO_4$, 0.015 M ProDOT-Bz_2 monomer and acetonitrile as a solvent. The polymerized potential was set at 1.55 V until the charge capacities were reached 25, 50, and 100 mC, respectively. The prepared PProDOT-Bz_2/30 s films were dipped in acetonitrile to wash out the unreacted ProDOT-Bz_2 monomer and were kept in an oven at 60 °C for 1 h.

2.3. Assembly of the DSSCs

The FTO glass was cleaned by sonicating it in acetone, ethanol, and deionized water for 10 min, respectively. 3 g titanium dioxide (TiO_2) powder, 4 mL deionized water, 0.05 mL acetylacetone (AcAc), 0.15 mL Triton X-100, and 2 mL graphene oxide (GO) were placed into bottles and stirred for 12 h. TiO_2 colloid was deposited on the FTO glass via the spin coating method at 1000 rpm for 11.5 s followed by coating at 2500 rpm for 15 s and was sintered at 450 °C in an annealing furnace for 30 min.

Afterwards, a TiO_2 mixture consisting of 0.25 g TiO_2 powder, 0.025 g iodine (I_2), and 25 mL AcAc was coated on the top of the TiO_2/GO layer by electrophoretic deposition [34]. Finally, the double-layer TiO_2 photoelectrode was annealed at 450 °C for 30 min again. The prepared film with an active area of 0.25 cm^2 was immersed in ethanol solution containing 0.5 mM N3 dye. The DSSC electrolyte consisted of 0.6 M DMPII, 0.5 M LiI, 0.05 M I_2, and 0.5 M TBP in 15 mL MPN. The as-prepared TiO_2 photoelectrode and CE were separated by a 65 μm thick Teflon tape filled with an electrolyte. The structure of dye-sensitized solar cells is shown in Figure 1.

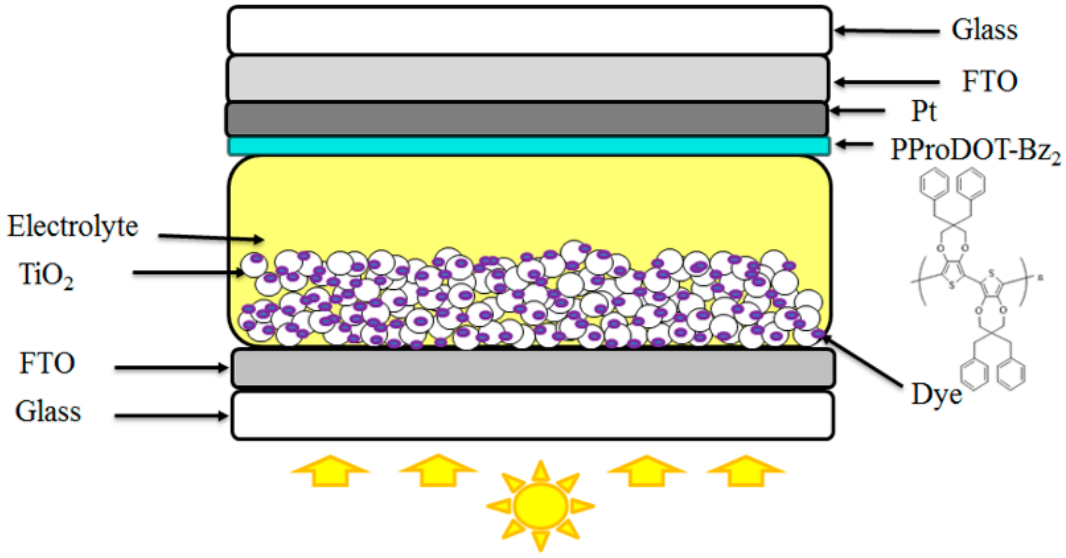

Figure 1. The structure of dye-sensitized solar cells.

2.4. Characterization

The photovoltaic performances of DSSCs were measured using a solar simulator (MFS-PV-Basic-HMT, Shulin, Taiwan) and the intensity of incident sunlight was 100 mW/cm^2. The Nyquist plot and electrochemical behavior of DSSC were investigated by electrochemical impedance spectroscopy (EIS, BioLogic SP-150, Seyssinet-Pariset, France), which were measured in the dark under a bias of −0.7 V. The frequency of EIS was set from 1 MHz to 50 mHz and an AC perturbation signal was set at 10 mV. The morphologies of CEs were observed by scanning electron microscope (SEM, JEOL JSM-7800F, Tokyo, Japan). Cyclic voltammetry measurements were implemented using a CHI660a electrochemical analyzer (CH Instruments, Austin, TX, USA).

3. Results and Discussion

3.1. Surface Morphology of the PProDOT-Bz$_2$ Film

The surface morphology of PProDOT-Bz_2/Pt composite films was studied using SEM images, as shown in Figure 2. Figure 2a shows the surface morphology of 30 s Pt–FTO glass; the surface morphologies of PProDOT-Bz_2 with 0.025, 0.05, and 0.1 charge capacity (0.025, 0.05, and 0.1 C/cm^2) polymerized on 30 s Pt–FTO glass are shown in Figure 2b–d, respectively. The SEM images indicate that the PProDOT-Bz_2/30 s Pt composite films exhibited a three-dimensional porous network structure, which means electroactive sites may have increased in the composite films for I_3^- to I^-. The porous morphology of PProDOT-Bz_2 film could facilitate the penetration of DSSC electrolyte, and the charge transfer resistance decreased at the CE/electrolyte interface [6]. The resultant porous structure of the PProDOT-Bz_2/30 s Pt composite films could also facilitate the penetration of the electrolyte in CEs of DSSCs, resulting in a reduced charge transfer resistance at the CE/electrolyte interface. However, the porous structure of the PProDOT-Bz_2/30 s Pt composite films decreased with the increasing charge

capacity until 0.1 C, a proper electron transfer process could not be expected from the substrate to the composite film and to the triiodide ions in DSSC electrolyte. Accordingly, the charge transfer efficiency of PProDOT-Bz_2/30 s Pt composite film decreased [35].

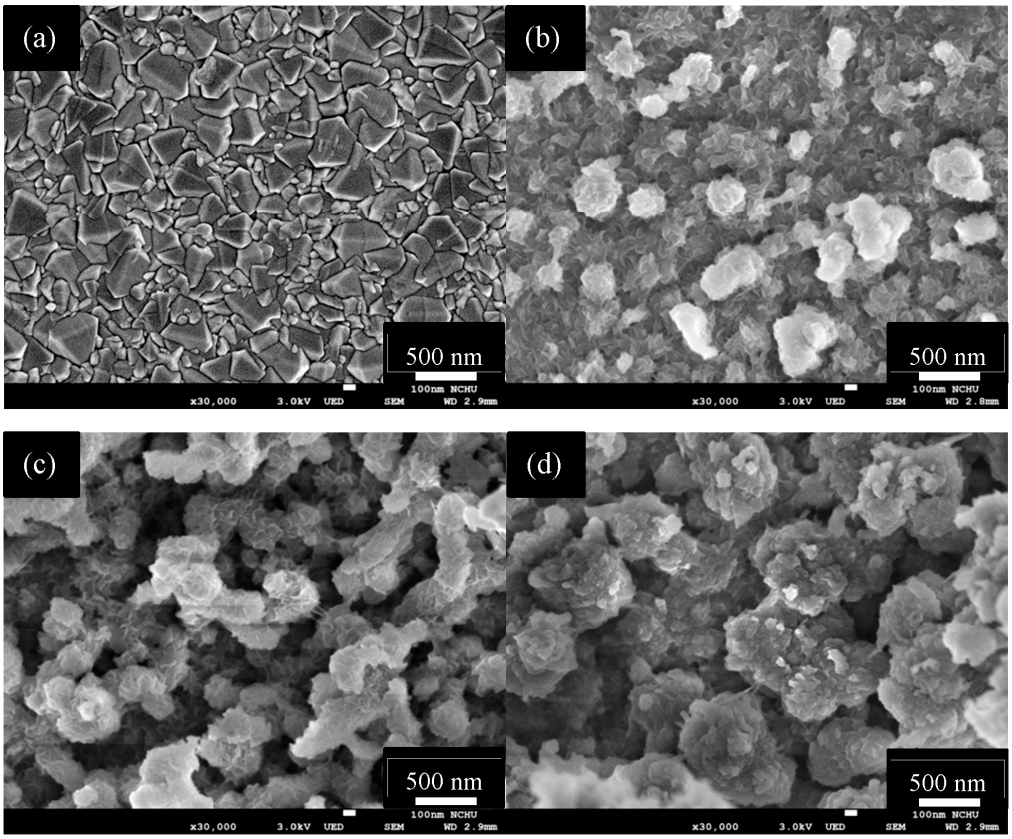

Figure 2. SEM images of the (**a**) 30 s Pt–FTO; (**b**) 0.025 C/cm^2 PProDOT-Bz_2/30 s Pt–FTO; (**c**) 0.05 C/cm^2 PProDOT-Bz_2/30 s Pt–FTO; (**d**) 0.1 C/cm^2 PProDOT-Bz_2/30 s Pt–FTO.

3.2. Photovoltaic Performances

Figure 3 shows the current density–voltage (*J*–*V*) curves of the DSSCs based on various CEs under AM 1.5 G (100 mW/cm^2) light illumination. The photovoltaic parameters such as the short-circuit current density (J_{sc}), open circuit voltage (V_{oc}), fill factor (F.F.) and photovoltaic conversion efficiency (η) are summarized in Table 1. The DSSC with sputtering time of 30 s Pt–FTO film showed lower efficiency (3.11%) than that sputtered for 360 s Pt–FTO film (3.58%). For the DSSCs fabricated with PProDOT-Bz_2/Pt composite films, the photovoltaic conversion efficiency increased from 3.33% to 3.50% as the charge capacity increased from 0.025 to 0.05 C/cm^2. As the charge capacity increased to 0.1 C/cm^2, the photovoltaic conversion efficiency decreased to 2.08%. 0.1 C/cm^2 PProDOT-Bz_2/30 s Pt CE-based DSSC showed lower photovoltaic conversion efficiency value than those of other CEs, this can be attributed to 0.1 C/cm^2 PProDOT-Bz_2/30 s Pt CE showing lower catalytic activity and lower surface area than those of other CEs, as confirmed by the SEM images in Figure 2. In addition, we also compared the photovoltaic performances of 0.05 C/cm^2 PProDOT-Bz_2/30 s Pt CE-based DSSC with 0.05 C/cm^2 PEDOT/30 s Pt CE-based DSSC. 0.05 C/cm^2 PProDOT-Bz_2/30 s Pt CE-based DSSC displays higher photovoltaic conversion efficiency value than that of 0.05 C/cm^2 PEDOT/30 s Pt CE-based DSSC.

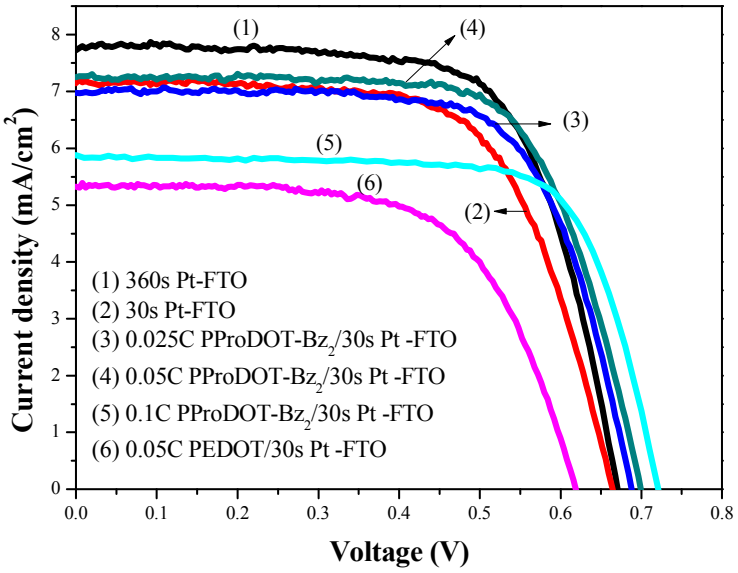

Figure 3. *J–V* curves of the DSSCs based on 360 s Pt, 30 s Pt, 0.025 C/cm^2 PProDOT-Bz$_2$/30 s Pt, 0.05 C/cm^2 PProDOT-Bz$_2$/30 s Pt, and 0.1 C/cm^2 PProDOT-Bz$_2$/30 s Pt counter electrodes, respectively. The DSSC electrolyte is based on 0.6 M DMPII, 0.5 M LiI, 0.05 M I_2, and 0.5 M TBP in 15 mL MPN.

Table 1. The photovoltaic parameters of DSSCs with various counter electrodes.

Counter Electrode	V_{oc} (V)	J_{sc} (mA/cm^2)	F.F. (%)	η (%)
360 s Pt	0.67 ± 0.02	7.80 ± 0.25	68.61 ± 2.77	3.58 ± 0.10
30 s Pt	0.67 ± 0.03	7.20 ± 0.31	64.94 ± 2.34	3.11 ± 0.11
0.025 C/cm^2 PProDOT-Bz$_2$/30 s Pt	0.69 ± 0.02	7.03 ± 0.45	68.82 ± 2.90	3.33 ± 0.11
0.05 C/cm^2 PProDOT-Bz$_2$/30 s Pt	0.70 ± 0.04	7.27 ± 0.35	68.74 ± 2.25	3.50 ± 0.13
0.1 C/cm^2 PProDOT-Bz$_2$/30 s Pt	0.62 ± 0.03	5.31 ± 0.33	64.46 ± 2.83	2.08 ± 0.13
0.05 C/cm^2 PEDOT/30 s Pt	0.72 ± 0.04	5.88 ± 0.28	73.09 ± 2.14	3.10 ± 0.14

3.3. Electrochemical Impedance Spectra

EIS analysis was employed to study the charge transfer resistances at the interface of the electrode. The Nyquist plots of the DSSC with different CEs in the measured frequency range from 1 to 50 MHz are shown in Figure 4, and their corresponding parameters are listed in Table 2. The R_s in the equivalent circuit corresponds to the ohmic series resistance of the substrate and its catalytic layer. The value could be evaluated by using the onset point of the first semicircle (left-hand side) in the high frequency region. A lower R_s refers to a better attachment of the catalytic film onto the substrate and therefore to a better conductivity of the film and better fill factor (F.F.) of the pertinent DSSC [18]. The first semicircle in the high-frequency zone of impedance spectra denotes the charge transfer resistance at CE/electrolyte interface (R_1), implying the catalytic properties of the CEs towards triiodide ion reduction [10]. A lower R_1 can be attributed to higher electrocatalytic activity from the reduction of I_3^- to I^-. The second semicircle in the middle-frequency region is related to the resistance at the TiO_2/dye/electrolyte (R_2). The third semicircle in the low-frequency region denotes the Warburg diffusion resistance of the electrolyte (W) [15]. DSSCs are fabricated using various CEs, the resistance between the CE and electrolyte (R_1) is a crucial parameter for the influence of various CEs. A lower R_1 can be ascribed to a higher electrocatalytic activity from the reduction of I_3^- to I^- at CE/electrolyte interface. 0.025 C/cm^2 PProDOT-Bz$_2$/30 s Pt–FTO and 0.05 C/cm^2 PProDOT-Bz$_2$/30 s Pt–FTO show lower R_1 values than that of 30 s Pt–FTO. These results may be attributed to the high conductivity and porous structure of these PProDOT-Bz$_2$/30 s Pt films that increased the electron transfer and facilitated the penetration of electrolyte in CEs of DSSCs [13].

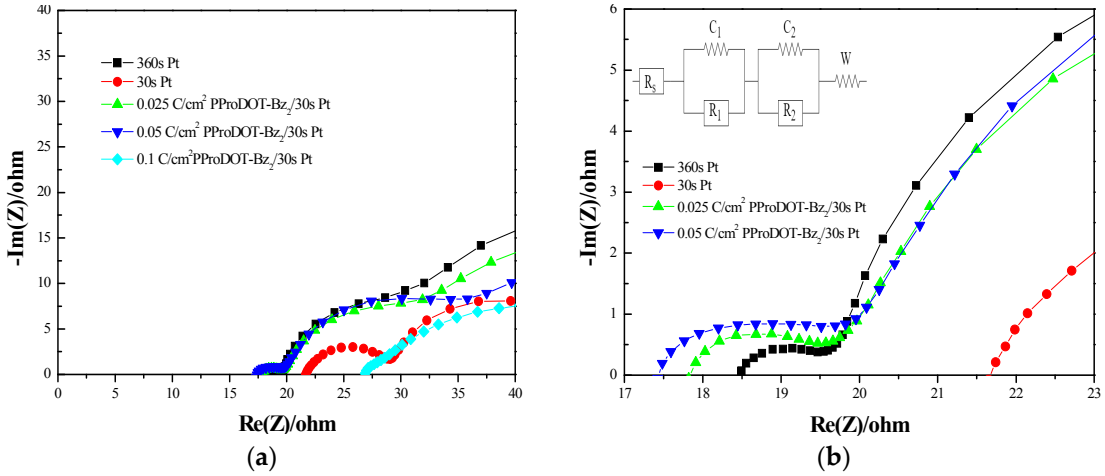

Figure 4. (**a**) Nyquist plots of the DSSCs based on 360 s Pt, 30 s Pt, 0.025 C/cm^2 PProDOT-Bz$_2$/30 s Pt, 0.05 C/cm^2 PProDOT-Bz$_2$/30 s Pt, and 0.1 C/cm^2 PProDOT-Bz$_2$/30 s Pt counter electrodes; (**b**) an enlarged graph of (**a**).

Table 2. The resistance and capacitance of equivalent circuit for DSSCs.

Counter Electrode	R_s (Ω)	C_1 (μF)	R_1(Ω)	C_2 (mF)	R_2 (Ω)
360 s Pt–FTO	18.42	85.63	1.05	5.12	12.57
30 s Pt–FTO	21.65	27.49	7.40	3.61	15.71
0.025 C/cm^2 PProDOT-Bz$_2$/30 s Pt–FTO	17.82	38.05	1.65	3.89	12.43
0.05 C/cm^2 PProDOT-Bz$_2$/30 s Pt–FTO	17.43	66.63	2.08	3.49	10.57
0.1 C/cm^2 PProDOT-Bz$_2$/30 s Pt–FTO	26.85	0.013	15.14	3.04	51.47

3.4. Cyclic Voltammetry

The electrochemical measurement of cyclic voltammetry (CV) was carried out using three electrode systems; various CEs were used as working electrodes, a platinum wire was used as a counter electrode, and Ag/AgCl was used as a reference electrode. The CV measurements were used to evaluate the electrocatalytic activities of 360 s Pt, 30 s Pt, and 0.05 C PProDOT-Bz$_2$/30 s Pt CEs in acetonitrile solution containing 0.1 M $LiClO_4$, 10 mM LiI, and 1 mM I_2. In general, the electrocatalytic activity of a CE is determined using two parameters, one is the separation of anodic and cathodic peak (ΔE_p), and the other is cathodic peak current density (I_{pc}). The overall electrocatalytic ability of CEs was characterized using these parameters. A larger I_{pc} denotes greater electrocatalytic ability, and a smaller ΔE_p indicates a lower overpotential toward the catalytic reduction of the triiodide ion to the iodide ion in DSSCs [10,25]. Compared with 30 s Pt CE as shown in Figure 5, 0.05 C PProDOT-Bz$_2$/30 s Pt CE exhibits a higher I_{pc} than that of 30 s Pt CE. In addition, these CEs show similar ΔE_p, indicating similar overpotentials toward the catalytic reduction of the triiodide ion to the iodide ion. 0.05 C PProDOT-Bz$_2$/30 s Pt CEs exhibits higher overall electrocatalytic ability than that of 30 s Pt CE, this may be attributed to 0.05 C PProDOT-Bz$_2$/30 s Pt composite films possess porous structure. High active area of porous structure facilitates the reduction reaction of I^-/I_3^-.

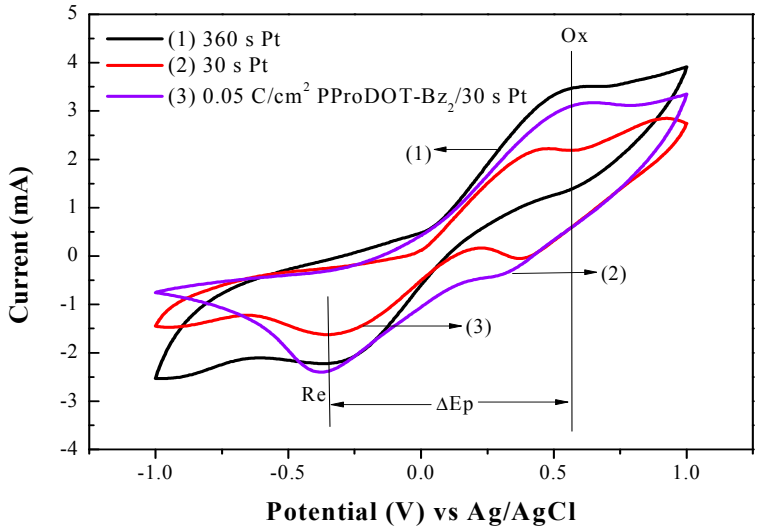

Figure 5. Cyclic voltammetry of the various counter electrodes at a scan rate of 100 mV s^{-1} in acetonitrile solution containing 0.1 M $LiClO_4$, 10 mM LiI, and 1 mM I_2.

4. Conclusions

Poly(3,3-dibenzyl-3,4-dihydro-2*H*-thieno[3,4-*b*][1,4]dioxepine)/platinum composite films (PProDOT-Bz_2/Pt) were used as the CEs in DSSCs. The DSSC based on 0.05 C PProDOT-Bz_2/30 s Pt composite CE exhibited a photovoltaic conversion efficiency of 3.50%, which was higher than that with 30 s Pt CE (3.11%) and up to 98% of that with 360 s Pt CE (3.58%) under the 100 mW/cm^2 light illumination. The results indicate that 0.05 C PProDOT-Bz_2/30 s Pt composite films represent a promising substitute for the expensive Pt as CE is for DSSC.

Acknowledgments: The authors would like to thank the Ministry of Science and Technology of Republic of China for financially supporting project MOST 103-2221-E-224-058-MY3 and MOST 104-2221-E-224-030.

Author Contributions: Jung-Chuan Chou, Yu-Chi Huang, and Tzi-Yi Wu designed and conceived the experiments; Yu-Chi Huang implemented the experiments; Jui-Cheng Chang, Yu-Chi Huang, Tzi-Yi Wu, Yi-Hung Liao, Chih-Hsien Lai, Chia-Ming Chu, and Yu-Jen Lin characterized the photovoltaic properties.

Conflicts of Interest: The authors declare no conflict of interest.

References

1. O'Regan, B.; Grätzel, M. A low-cost, high-efficiency solar cell based on dye-sensitized colloidal TiO_2 films. *Nature* **1991**, *353*, 737–740. [CrossRef]
2. Tsao, M.H.; Wu, T.Y.; Wang, H.P.; Sun, I.W.; Su, S.G.; Lin, Y.C.; Chang, C.W. An efficient metal free sensitizer for dye-sensitized solar cells. *Mater. Lett.* **2011**, *65*, 583–586. [CrossRef]
3. Che Balian, S.R.; Ahmad, A.; Mohamed, N.S. The effect of lithium iodide to the properties of carboxymethyl κ-carrageenan/carboxymethyl cellulose polymer electrolyte and Dye-sensitized solar cell performance. *Polymers* **2016**, *8*, 163. [CrossRef]
4. Wu, T.Y.; Tsao, M.H.; Chen, F.L.; Su, S.G.; Chang, C.W.; Wang, H.P.; Lin, Y.C.; Ou-Yang, W.C.; Sun, I.W. Synthesis and characterization of organic dyes containing various donors and acceptors. *Int. J. Mol. Sci.* **2010**, *11*, 329–353. [CrossRef] [PubMed]
5. Dzulkurnain, N.A.; Ahmad, A.; Mohamed, N.S. P(MMA–EMA) random copolymer electrolytes incorporating sodium iodide for potential application in a Dye-sensitized solar cell. *Polymers* **2015**, *7*, 266–280. [CrossRef]
6. Wu, T.Y.; Tsao, M.H.; Chen, F.L.; Su, S.G.; Chang, C.W.; Wang, H.P.; Lin, Y.C.; Sun, I.W. Synthesis and characterization of three organic dyes with various donors and rhodanine ring acceptor for use in dye-sensitized solar cells. *J. Iran. Chem. Soc.* **2010**, *7*, 707–720. [CrossRef]

7. Sun, I.W.; Wang, H.P.; Teng, H.; Su, S.G.; Lin, Y.C.; Kuo, C.W.; Chen, P.R.; Wu, T.Y. Cyclic ammonium-based ionic liquids as potential electrolytes for dye-sensitized solar cells. *Int. J. Electrochem. Sci.* **2012**, *7*, 9748–9764.
8. Wu, T.Y.; Tsao, M.H.; Su, S.G.; Wang, H.P.; Lin, Y.C.; Chen, F.L.; Chang, C.W.; Sun, I.W. Synthesis, characterization and photovoltaic properties of di-anchoring organic dyes. *J. Braz. Chem. Soc.* **2011**, *22*, 780–789. [CrossRef]
9. Theerthagiri, J.; Senthil, A.R.; Madhavan, J.; Maiyalagan, T. Recent progress in non-platinum counter electrode materials for dye-sensitized solar cells. *Chem. Electron. Chem.* **2015**, *2*, 928–945. [CrossRef]
10. Bora, C.; Sarkar, C.; Mohan, K.J.; Dolui, S. Polythiophene/graphene composite as a highly efficient platinum-free counter electrode in dye-sensitized solar cells. *Electrochim. Acta* **2015**, *157*, 225–231. [CrossRef]
11. Yun, S.; Lund, P.D.; Hinsch, A. Stability assessment of alternative platinum free counter electrodes for dye-sensitized solar cells. *Energy Environ. Sci.* **2015**, *8*, 3495–3514. [CrossRef]
12. Jeon, S.S.; Kim, C.; Lee, T.H.; Lee, Y.W.; Do, K.; Ko, J.; Im, S.S. Camphorsulfonic acid-doped polyaniline transparent counter electrode for dye-sensitized solar cells. *J. Phys. Chem. C* **2012**, *116*, 22743–22748. [CrossRef]
13. Qiu, Y.; Lu, S.; Wang, S.; Zhang, X.; He, S.; He, T. High-performance polyaniline counter electrode electropolymerized in presence of sodium dodecyl sulfate for dye-sensitized solar cells. *J. Power Sources* **2014**, *253*, 300–304. [CrossRef]
14. Chen, L.; Guo, C.X.; Zhang, Q.; Lei, Y.; Xie, J.; Ee, S.; Guai, G.; Song, Q.; Li, C.M. Graphene quantum-dot-doped polypyrrole counter electrode for high-performance dye-sensitized solar cells. *ACS Appl. Mater. Interfaces* **2013**, *5*, 2047–2052. [CrossRef] [PubMed]
15. Heo, S.Y.; Koh, J.K.; Kim, J.K.; Lee, C.S.; Kim, J.H. Three-dimensional conducting polymer films for Pt-free counter electrodes in quasi-solid-state dye-sensitized solar cells. *Electrochim. Acta* **2014**, *137*, 34–40. [CrossRef]
16. Kim, H.; Veerappan, G.; Park, J.H. Conducting polymer coated non-woven graphite fiber film for dye-sensitized solar cells: superior Pt-and FTO-free counter electrodes. *Electrochim. Acta* **2014**, *137*, 164–168. [CrossRef]
17. Han, R.; Lu, S.; Wang, Y.; Zhang, X.; Wu, Q.; He, T. Influence of monomer concentration during polymerization on performance and catalytic mechanism of resultant poly(3,4-ethylenedioxythiophene) counter electrodes for dye-sensitized solar cells. *Electrochim. Acta* **2015**, *173*, 796–803. [CrossRef]
18. Chen, P.-Y.; Li, C.-T.; Lee, C.-P.; Vittal, R.; Ho, K.-C. PEDOT-decorated nitrogen-doped graphene as the transparent composite film for the counter electrode of a dye-sensitized solar cell. *Nano Energy* **2015**, *12*, 374–385. [CrossRef]
19. Ke, C.-R.; Chang, C.-C.; Ting, J.-M. Modified conducting polymer films having high catalytic activity for use as counter electrodes in rigid and flexible dye-sensitized solar cells. *J. Power Sources* **2015**, *284*, 489–496. [CrossRef]
20. Seo, H.; Son, M.-K.; Itagaki, N.; Koga, K.; Shiratani, M. Polymer counter electrode of poly(3,4-ethylenedioxythiophene):poly(4-styrenesulfonate) containing TiO_2 nano-particles for dye-sensitized solar cells. *J. Power Sources* **2016**, *307*, 25–30. [CrossRef]
21. Yeh, M.-H.; Lee, C.-P.; Lin, L.-Y.; Nien, P.-C.; Chen, P.-Y.; Vittal, R.; Ho, K.-C. A composite poly(3,3-diethyl-3,4-dihydro-2*H*-thieno-[3,4-*b*][1,4]-dioxepine) and Pt film as a counter electrode catalyst in dye-sensitized solar cells. *Electrochim. Acta* **2011**, *56*, 6157–6164. [CrossRef]
22. Kang, G.; Choi, J.; Park, T. Pt-free counter electrodes with carbon black and 3D network epoxy polymer composites. *Sci. Rep.* **2016**, *6*, 22987. [CrossRef] [PubMed]
23. Bella, F.; Galliano, S.; Falco, M.; Viscardi, G.; Barolo, C.; Gratzel, M.; Gerbaldi, C. Approaching truly sustainable solar cells by the use of water and cellulose derivatives. *Green Chem.* **2017**, *19*, 1043–1051. [CrossRef]
24. Bella, F.; Pugliese, D.; Zolin, L.; Gerbaldi, C. Paper-based quasi-solid dye-sensitized solar cells. *Electrochim. Acta* **2017**, *237*, 87–93. [CrossRef]
25. Gemeiner, P.; Peřinka, N.; Švorc, L.; Hatala, M.; Gál, L.; Belovičová, M.; Syrový, T.; Mikula, M. Pt–free counter electrodes based on modified screen-printed PEDOT:PSS catalytic layers for dye-sensitized solar cells. *Mater. Sci. Semicond. Process.* **2017**, *66*, 162–169. [CrossRef]
26. Gerosa, M.; Sacco, A.; Scalia, A.; Bella, F.; Chiodoni, A.; Quaglio, M.; Tresso, E.; Bianco, S. Toward totally flexible Dye-sensitized solar cells based on titanium grids and polymeric electrolyte. *IEEE J. Photovolt.* **2016**, *6*, 498–505. [CrossRef]

27. Imperiyka, M.; Ahmad, A.; Hanifah, S.A.; Bella, F. A UV-prepared linear polymer electrolyte membrane for dye-sensitized solar cells. *Phys. Rev. B* **2014**, *450*, 151–154. [CrossRef]
28. Pavithra, N.; Velayutham, D.; Sorrentino, A.; Anandan, S. Thiourea incorporated poly(ethylene oxide) as transparent gel polymer electrolyte for dye sensitized solar cell applications. *J. Power Sources* **2017**, *353*, 245–253. [CrossRef]
29. Shanti, R.; Bella, F.; Salim, Y.S.; Chee, S.Y.; Ramesh, S.; Ramesh, K. Poly(methyl methacrylate–*co*–butyl acrylate–*co*–acrylic acid): Physico–chemical characterization and targeted dye sensitized solar cell application. *Mater. Des.* **2016**, *108*, 560–569. [CrossRef] [PubMed]
30. Chae, H.; Song, D.; Lee, Y.-G.; Son, T.; Cho, W.; Pyun, Y.B.; Kim, T.-Y.; Lee, J.H.; Fabregat-Santiago, F.; Bisquert, J.; et al. Chemical effects of tin oxide nanoparticles in polymer electrolytes-based Dye-sensitized solar cells. *J. Phys. Chem. C* **2014**, *118*, 16510–16517. [CrossRef]
31. Wu, T.Y.; Liao, J.W.; Chen, C.Y. Electrochemical synthesis, characterization and electrochromic properties of indan and 1,3-benzodioxole-based poly(2,5-dithienylpyrrole) derivatives. *Electrochim. Acta* **2014**, *150*, 245–262. [CrossRef]
32. Wu, T.Y.; Su, Y.S. Electrochemical synthesis and characterization of a 1,4-benzodioxan-based electrochromic polymer and its application in electrochromic devices. *J. Electrochem. Soc.* **2015**, *162*, 103–112. [CrossRef]
33. Wu, T.Y.; Chung, H.H. Applications of tris(4-(thiophen-2-yl)phenyl)amine-and dithienylpyrrole-based conjugated copolymers in high-contrast electrochromic devices. *Polymers* **2016**, *8*, 206. [CrossRef]
34. Chou, J.-C.; Lin, S.-C.; Liao, Y.-H.; Hu, J.-E.; Chuang, S.-W.; Huang, C.-H. The influence of electrophoretic deposition for fabricating dye-sensitized solar cell. *J. Nanomater.* **2014**, *2014*, 1–7. [CrossRef]
35. Li, C.-T.; Lee, C.-T.; Li, S.-R.; Lee, C.-P.; Chiu, I.T.; Vittal, R.; Wu, N.-L.; Sun, S.-S.; Ho, K.-C. Composite films of carbon black nanoparticles and sulfonated-polythiophene as flexible counter electrodes for dye-sensitized solar cells. *J. Power Sources* **2016**, *302*, 155–163. [CrossRef]